JOURNAL OF MATERIALS SCIENCE 31 (1996) 3167–3172

Finite element modelling of crack propagation in elastic–plastic media

Part I *Vertical surface breaking cracks*

K. SADEGHIPOUR, G. BARAN*, Z. FU, S. JAYARAMAN
Department of Mechanical Engineering, Temple University, Philadelphia, PA 19122 and
**School of Dentistry, Temple University, Philadelphia, PA 19140, USA*

Materials which are cyclically stressed by sliding indenters often undergo fatigue wear, as surface breaking vertical cracks and subsurface horizontal cracks propagate causing eventual loss of material. In this study, the authors model crack propagation in an elastic–plastic material using finite element techniques, and consider the influence of friction, elasticity, plasticity and degree of penetration on the *J*-integral at the tip of a vertical crack. Crack propagation directions are estimated using *J*-integral maxima as the determining variable. It is found that the *J*-integral values, as a measure of strain energy release rate, can be used to estimate the crack propagation angle. Its main advantage lies in the fact that it considers both modes (I, II) of crack propagation. Using the *J*-integral values, one finds that, in the absence of friction between the indenter and the material, the vertical crack is equally prone to propagation at both 45 and 135° angles. However, one notices that the vertical crack favours the direction opposite to the direction of rolling for non-zero values of friction, i.e. 135°. The effects of both the crack depth and the crack tip plasticity are also investigated. It is found that any experimental findings suggestive of crack orientations closer to the horizontal in the direction opposite to the sliding direction are probably a result of shallow vertical asperities or higher crack tip plasticity.

1. Introduction

In the clinical biomedical sciences, polymers and polymer composites are used often as dental restorative materials, replacing traditional metallic restorations. In time, these materials undergo fatigue wear, and require replacement [1, 2]. It is therefore of interest to develop a predictive model for fatigue-induced wear of these materials that would allow rapid material evaluation. In this portion of an ongoing study, the authors generate a finite-element model for fatigue crack propagation as a preliminary step to proposing a predictive wear model. The cusp of an opposing tooth sliding over the restorative material surface during chewing is simulated. As a first approximation, one assumes the restorative material surface to be smooth, and the opposing cusp is modelled as a cylinder with radius, R, allowing a two-dimensional axisymmetric model to be employed. One is at first specifically interested in the polymer matrix material, usually an epoxy-type thermoset.

A considerable body of analytical and experimental studies has been completed with the goal of predicting the contact fatigue life of mechanical components. Many of these investigations have been carried out to clarify the mechanism of rolling contact fatigue. However, controversy still persists regarding the mechanics of fatigue crack initiation and propagation, and one's understanding of these phenomena in polymers, with their time-dependent and elastic–plastic stress–strain behaviour, is incomplete.

Since the delamination theory of wear was introduced by Suh [3], a number of investigations have shown that wear sheets in sliding wear are formed as a result of subsurface deformation, crack nucleation and crack propagation. Fleming and Suh [4] were the first to analyse the propagation of a subsurface crack parallel to the surface using a linear elastic fracture mechanics (LEFM) approach. This treatment was based on the assumption that in the case of a horizontal subsurface crack, only the crack tip behind the moving asperity extends due to cyclic loading, since the crack is subjected to tensile stresses.

More recently, Rosenfield [5] did a similar analysis and added the effect of friction on the two crack faces in contact. Keer and coworkers [6] analysed surface and subsurface cracks under general Hertzian loading. Ghosn [7] studied the surface crack under mixed-mode loading and with tensile stress edge boundary conditions using the boundary integral method.

A controversial aspect of crack propagation studies of the past is the use of LEFM and the specific boundary conditions. When linear elastic fracture mechanics are used to predict rate of crack propagation under cyclic loading, the prerequisites are that the change in

0022–2461

the stress intensity factor be larger than a critical value called the threshold value, and that the plastic zone at the crack tip is small. As Sin and Suh [8] indicated, the major shortcoming of some earlier contributions is the use of LEFM, when the actual plastic zone surrounding the crack tip is large and extends to the surface. When the plastic zone size at the crack tip extends to a stress-free boundary, the stress intensity loses any physical significance. In short, not only is the stress intensity factor too small to enable crack propagation, but the plastic zone size is too large as well. Therefore, it is necessary to analyse the full elastic–plastic deformation of the crack tip.

In the past, only the propagation of a crack under simple loading conditions has been studied using LEFM. Three criteria are commonly used in predicting crack propagation directions: the maximum hoop stress criterion, the minimum strain energy density criterion and the maximum shear stress criterion. The maximum hoop stress criterion has been applied to predict the crack extension direction within an elastic medium [9]. Similar results are also obtained using the energy criterion [10]. However, this finding is based on elastic solutions, and therefore may be irrelevant to problems concerning elastic–plastic materials, unless the actual plastic stress components are proportional to the corresponding elastic stress components used for the prediction. At any rate, these criteria cannot be used to explain crack propagation when cracks are under compressive and shear loading.

Based on the experimental results of Jahanmir *et al.* [11], which showed that subsurface cracks propagate parallel to the surface for a considerable distance before they change direction, and observations that slip planes are shown to line up parallel to the surface in sliding wear, Suh argued that the maximum shear stress direction of these planes was likely to be the crack propagation direction, even though it was realized that it was difficult to determine where maximum shear stress was, since the entire region of interest was in the plastic range [12]. The solution was to examine the stress history and choose the shear stress location where yielding first occurred.

In sliding wear there are several experimental aspects of crack propagation that need to be understood: where the moving load is located with respect to a crack, when a vertical surface or a subsurface crack begins to propagate, the direction the crack is favoured to take, and how a crack's behaviour is effected by factors such as crack depth, friction and crack geometry. Experiments show that many cracks propagate parallel to the surface and ultimately change their direction toward the surface, terminating their growth. In delamination wear only the crack tip at the trailing side reaches the surface. These prior investigations do not provide satisfactory solutions for the problem, which involves indentation of an elastic–plastic material followed by indenter sliding.

This paper does not try to address all the above issues. The scope of the present analysis is rather modest. Here, information produced in a previous work [12] on static microindentation (specifically material modelling, and the location and formation of different cracks), is used and applied to a sliding cylinder model when surface breaking vertical cracks exist. These surface cracks may be produced under different circumstances during material preparation, testing or finishing phases. It is the purpose of this paper to use these simple models to assess crack propagation, crack orientation and crack interaction.

1.1. Theoretical background

The basic principles derived from static indentation fracture theory are still useful in understanding crack initiation and propagation in wear testing, even though the existence of a crack and the motion of the indenter sliding on the material surface affects stress distribution patterns.

The constitutive model for the specimen material was based on a series of experimental microindentation tests which were reported in a previous publication [12]. Material response was simplified to be similar to a bilinear elastic–plastic Von Mises material. As an indenter contacts the surface, the applied load is distributed over the contact site as compressive stresses. Elastic deformation of the material, both at and around the contact site, gives rise to tensile stresses confined to a shallow "skin" outside this region, and compressive stresses immediately below. The combination of tensile and compressive stresses causes the formation of ring, median and radial cracks when spherical indentors are considered [12].

During the initial penetration, the stress field is usually described by three components: stresses radiating from the point of contact (radial stresses), stresses which encircle the contact (hoop stresses) and shear stresses. It is the behaviour of these stresses in the immediate vicinity of the contact (the so-called "near-field" stresses) which determine the point of initiation of indentation-induced cracks. Stresses at points far removed from the contact (the "far-field" stresses) also determine the path of propagation of the same cracks. All analyses were performed using the existing package, ADINA 6.1 [13]. ADINA was chosen due to its capabilities of plastic analysis, contact mechanics analysis and fracture mechanics analysis.

In previous studies, stress intensity factors (K_{I}, K_{II} and K_{III}) were usually chosen to describe the fracture behaviour in elastic fields. It is indeed the use of the stress intensity factor as the characterizing parameter for crack extension that is a fundamental principle of LEFM. However, the elastic distribution in the vicinity of a crack tip causes a stress singularity at the crack tip; thus the elastic solution is not unconditionally applicable.

The J-integral is a generally accepted parameter to describe fracture behaviour in an elastic–plastic field. It is defined as

$$J = \int_{\Gamma} \left(W \, \mathrm{d}x_2 - \sigma_{ij} \frac{\partial u_i}{\partial x_i} n_j \mathrm{d}s \right) \qquad (1)$$

where Γ is the line contour enclosing the crack tip; x_i the Cartesian co-ordinates; σ_{ij}, components of stress tensor; u_i, components of the displacement vector; n_j, components of unit vector normal to Γ; d_s, length of increment along Γ; and $W = \int \sigma_{ij} d\varepsilon_{ij}$, i.e. total stress work density (per unit volume). For linear elastic materials, Equation 1 is related to stress intensity factors as

$$J = \frac{K_{\mathrm{I}}^2}{E'} + \frac{K_{\mathrm{II}}^2}{E'} + \frac{K_{\mathrm{III}}^2}{G} \qquad (2)$$

where $E' = E$ in plane stress, and $E' = E/(1 - \nu^2)$ in plane strain.

In the present investigation, the "line contour" method is used to determine the cylinder location when crack initiation could occur [13]. This method is used in a two-dimensional analysis to calculate the J-integral, a contour independent parameter characterizing the severity of the displacement, and stress and strain field at the tip of the crack. When used in conjunction with finite element models, the line contour is defined by a series of adjoining segments passing through the elements located on the contour. The integration of the J-integral along each segment is performed numerically using the value of the variables at the integration points which define the segment.

According to principles of fracture mechanics, all stress systems in the vicinity of a crack tip may be derived from three modes of loading, i.e. opening mode, sliding mode and tearing mode. The line contour method can reflect a realistic composition of those three modes because it is not necessary to verify a virtual displacement of a domain around the crack tip against a virtual extension method.

In contrast, the "virtual crack extension" method can only be used to determine the possible crack propagation direction. In this method, a small domain around a crack tip and its virtual possible extension direction must be specified a priori. This virtual extension direction is not always true during cylinder sliding from one side of the crack to the other, but it is true when the cylinder reaches a location at which the J-integral has maximum value. In other words, when a cylinder slides on a specimen surface, different potenital crack propagation directions exist depending on the cylinder location. Further, there is a most likely crack propagation direction for each cylinder location. Therefore, this method can be used to evaluate the J-integral of a given body with pre-existing cracks.

The total potential energy variation is calculated using a "virtual material shift" obtained by shifting the nodes of a domain that includes at least one of the crack's front nodes. The equivalence between the J-integral and the ratio of the total potential energy variations to the crack area increase holds only for linear elastic and elastic–plastic analyses when the deformation theory of plasticity is applicable.

Once the ADINA finite element model is developed, the expression of the energy release rate is presented as

$$G = \frac{1}{A_c}\int_v \left[\left(\sigma_{ij}\frac{\partial u_j}{\partial x_k} - W\delta_{ik}\right)\frac{\partial \Delta x_k}{\partial x_i} - f_i\frac{\partial u_i}{\partial x_j}\Delta x_j\right] dv - \frac{1}{A_c}\int_s t_i\frac{\partial u_i}{\partial x_j}\Delta x_j ds \qquad (3)$$

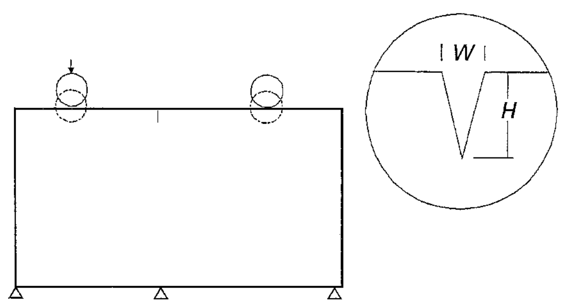

Figure 1 Schematic of the sliding cylinder contact problem with a vertical surface crack: W, width; H, height of crack.

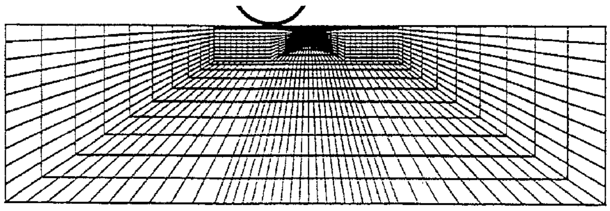

Figure 2 Finite element mesh of the vertical surface crack model.

where v and s are the volume and surface of the cracked body, respectively; Δx_k are components of the virtual crack extension vector; A_c is the increase in crack area; δ_{ij}, Kronecker's delta; f_i, components of the body force vector; t_i, components of the surface tension vector; and $W = \int_0^{\varepsilon_{ij}} \sigma_{ij} d\varepsilon_{ij}$, i.e. the total stress work density.

The schematic of the model is shown in Fig. 1. The finite element model is made of eight node, isoparametric plain strain quadratic elements capable of handling very large displacements with elasto–plastic properties (Fig. 2). The cylinder is assumed to be rigid and no body and/or inertia forces are included. During this isothermal process, the loading was considered to be monotonic and proportional, and the material properties were considered to be homogeneous. For the purpose of generality the finite element analysis was considered to be dimensionless, but there was no reason in principal why it could not be related to the present experimental studies.

2. Results and discussion

Fig. 3a shows the variation of the J-integral surrounding the crack tip with crack propagation angle, θ, for two different values of the elastic modulus, E ($E_{\mathrm{VE}} = 3E_{\mathrm{VB}}$), for a vertical crack. As the J-integral is a measure of the strain energy release rate, Fig. 3a thus indicates the possible strain energy release rate if the crack chooses to propagate at an angle θ (virtual crack propagation angle). The angle at which the maximum strain energy release rate occurs is the prospective crack propagation direction. As seen in Fig. 3a, there is a distinct increase in the J-integral value at the same angle. Fig. 3b shows the J-integral values corresponding to different cylinder locations assuming the crack propagates along its initial orientation. However, since the J-integral value depends on the virtual crack propagation angle, the crack may

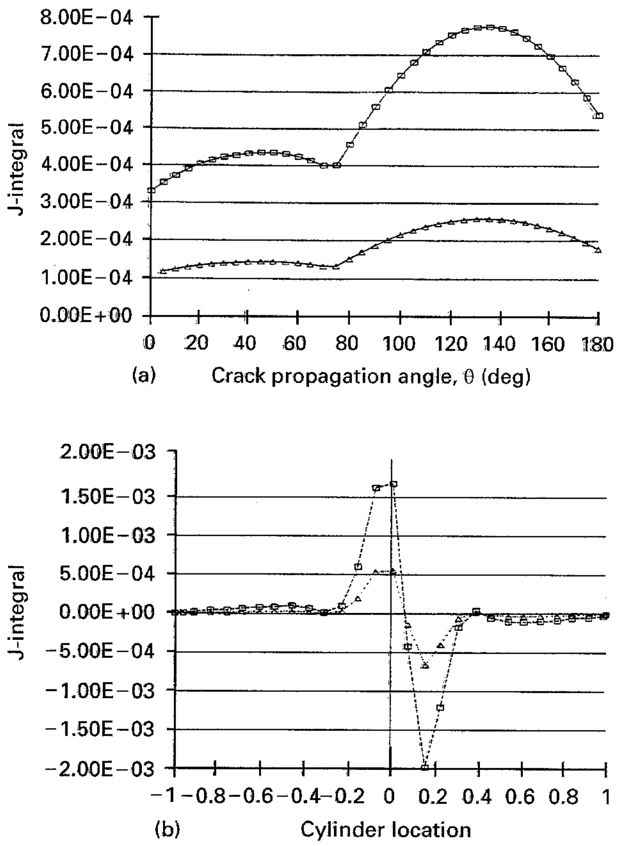

Figure 3 The plots of J-integral versus: (a) the crack propagation angle, and (b) the cylinder location, for different elastic moduli, i.e. $E_{VE} = 3E_{VB}$.(△) VB, (⊟) VE.

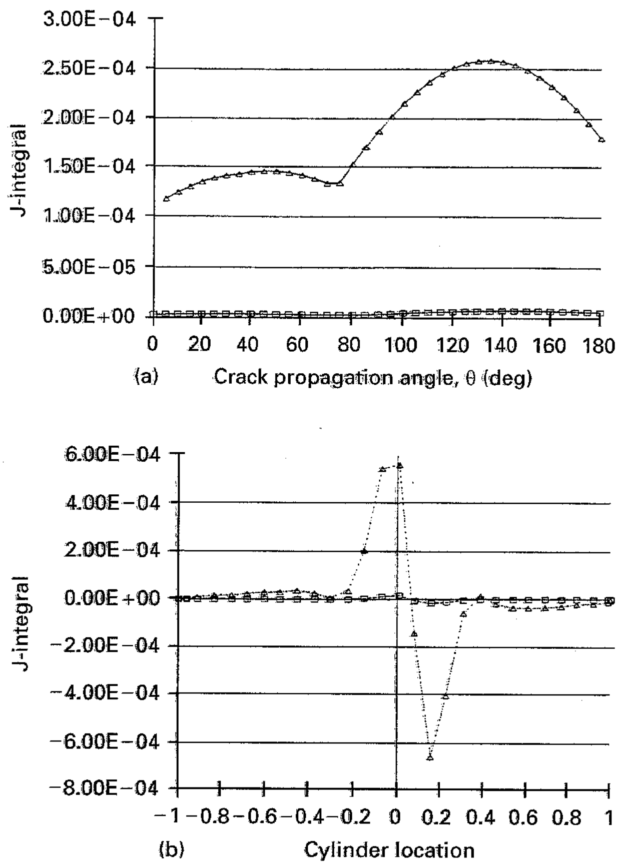

Figure 4 The plots of J-integral versus: (a) the crack propagation angle, and (b) the cylinder location, for different down load (△, VB = 3 per cent R, and, ⊟, VL = 0.5 per cent R).

not propagate at the location at which peak J-integral values occur.

When the indentation displacement is decreased from 3 (VB) to 0.5 per cent (VD2) of R, where R is the radius of the cylinder indenting the half-space, the J-integral values approach zero (see Fig. 4a). The J-integral corresponding to each angle is the maximum J-integral value at the same angle for different cylinder locations. Fig. 4b, which shows the J-integral values obtained by the contour integration method, clearly indicates that there is a sharp increase only when the cylinder approaches close to the surface crack for the case of 3 per cent R applied displacement. The crack tip field seems to be relatively undisturbed when the applied cylinder displacement reduces to 0.5 per cent R.

The effect of friction between the indenter and the sliding surface yields results shown in Fig. 5a. In the absence of friction (VF0), the vertical crack is equally prone to propagation at both the 45 and 135° angles. However, the vertical crack favours the direction opposite to the direction of rolling for non-zero values of friction, i.e., when the friction coefficient μ is one of these values: 0.03 (VF3), 0.06 (VF6), 0.09 (VF9) or 0.27 (VF27). This preferred crack propagation angle is 135° measured clockwise with respect to the horizontal line in the direction of rolling. Friction appears to have little effect on the strain energy release rate when the crack propagates along its initial orientation as shown in Fig. 5b.

When the depth of a vertical crack, H, increases from 2 (VD2) to 20 per cent (VB) of R, the J-integral

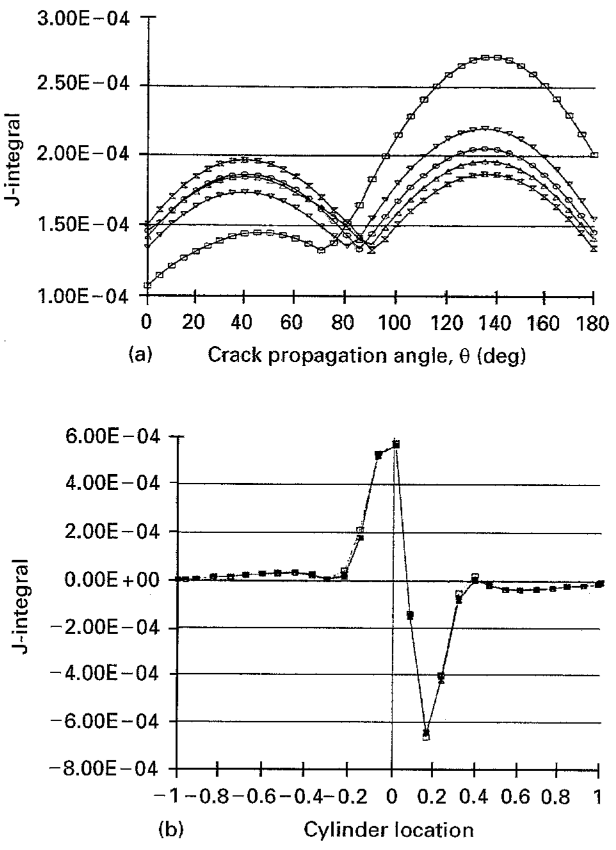

Figure 5 The plots of J-integral versus: (a) the crack propagation angle, and (b) the cylinder location, for different friction coefficients. (⊠) $\mu_{VF0} = 0$, (△) $\mu_{VF3} = 0.03$, (⊖) $\mu_{VF6} = 0.06$, (▽) $\mu_{VF9} = 0.09$ and (⊟) $\mu_{VF27} = 0.27$.

variation with θ is shown in Fig. 6a. The behaviour is different from the effects studied above, in that both the magnitude of the J-integral and the crack propagation direction change. This direction changes from 95 to 135° as the crack depth decreases to 2 per cent R from an initial 20 per cent R. This suggests that an initially shallow vertical crack would initially tend to grow more towards the horizontal in the direction opposite to sliding. As the crack length increases, it would tend to grow towards the vertical direction. This interpretation of the results of Fig. 6a does not account for the possible effects of crack kinks. The J-integral variation, obtained by the contour integration method, with cylinder location for two different crack tip depths is shown in Fig. 6b.

As mentioned earlier, Ghosn [7] has analysed surface crack propagation in a rotating inner raceway of a high speed roller bearing using the boundary integral method. Ghosn's analysis suggests that a vertical surface crack would propagate initially at an angle of 71° to the vertical, opposing the rolling direction. Keer *et al.* [6] suggest a crack propagation direction of about 69° from the vertical for a similar surface crack. Both these workers have used LEFM techniques in their analyses. These higher values, compared to the findings of the present study which suggest a crack propagation direction of 45° from the vertical, are due probably to the lower vertical crack lengths with respect to the cylinder radius analysed by these workers. Also, Ghosn has ignored the K_{II} crack propagation mode by using the maximum tangential stress theory. The theory used in the present study includes both K_{I} and K_{II} modes. This is because the J-integral value is a function of both modes of crack propagation as described by Equation 4, when LEFM is valid

$$J = \frac{\beta}{E}(K_{\mathrm{I}}^2 + K_{\mathrm{II}}^2) \qquad (4)$$

where $\beta = 1 - v^2$ for plane strain and $\beta = 1$ for plane stress. The present study ignores the effect of the alternating stress field, and thus the alternating J-integral values, as the cylinder moves from one end to another. This assumption is reasonable since the J-integral is not a true measure of the propensity for crack propagation once unloading begins. The crack tip is typically subject to a sequence of loading–unloading cycles during the cylinder movement on the surface. As the J-integral values are initially zero when the cylinder is farthest away from the crack tip, the angle at which the maximum J-integral value occurs would be the direction in which the crack most likely propagates. Citing Ghosn [7, Fig. 5 therein], both the initial and the overall (straight line fit) experimental crack propagation direction is close to or less than 45° from the vertical opposing the rolling direction. This angle is closer to the findings of the present study.

One other important factor that needs to be considered in comparing the experimental and calculated crack propagation angles is the effect of the crack tip plastic zone. This is illustrated in Fig. 7a. As seen, the

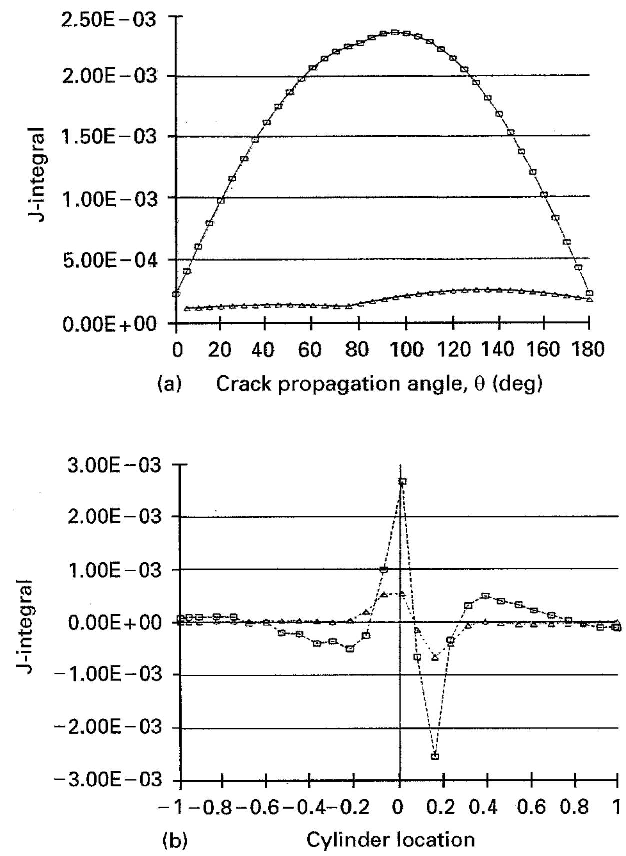

Figure 6 The plots of J-integral versus: (a) the crack propagation angle, and (b) the cylinder location, for different crack tip depth. (△) $H_{\mathrm{VB}} = 15$ per cent R, and (⊟) $H_{\mathrm{VD2}} = 2$ per cent R, when R is the radius of the cylinder.

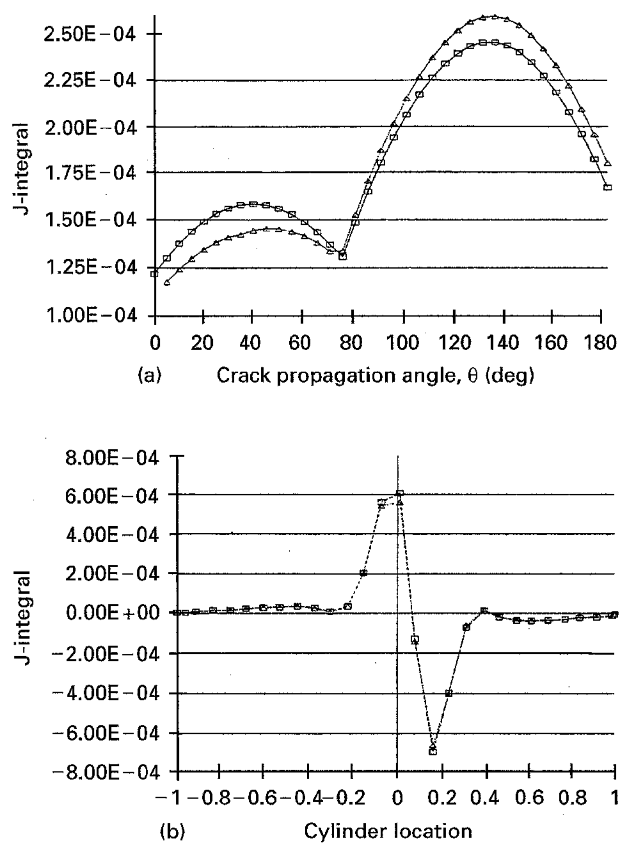

Figure 7 The plots of J-integral versus: (a) the crack propagation angle, and (b) the cylinder location, for different crack geometries. (△) $H/W = 75$ for VB, and (⊟) $H/W = 5$ for VS.

maximum J-integral value occurs at higher values of θ when plastic deformation increases. Thus, any experimental finding suggestive of crack orientations closer to the horizontal in the direction opposite to rolling direction (higher θ values) is probably a result of shallow vertical asperities or higher crack tip plasticity. Once again, it is assumed that the effect of neighbouring asperities is negligible.

3. Conclusions

In conclusion, J-integral values were used to estimate the crack propagation angle at the tip of the vertical crack and to calculate the location of the cylinder. The J-integral application proved to be more advantageous than using the critical intensity factor values since it considered both modes (I and II) of crack propagation. Also, as J-integral values were used, the effect of crack tip plasticity was accounted for. Pin-on-disc experiments on polymeric restorative materials are currently being done to induce fatigue crack propagation in these materials. These will allow verification of predicted crack propagation directions.

Acknowledgements

This research is supported by NIH grant No. DE-09530.

References

1. J. L. DRUMMOND, *J. Oral Rehabilitation* **6** (1989) 509.
2. P. G. T. van DER VAST, P. L. M. LEMMENS, M. C. R. B. PETERS and A. J. M. PLASSCHAERT, *J. Biomech.* **24** (1991) 341.
3. N. P. SUH, *Wear* **25** (1973) 111.
4. J. R. FLEMING and N. P. SUH, *ibid.* **44** (1979) 39.
5. A. R. ROSENFIELD, *ibid.* **61** (1980) 125.
6. L. M. KEER, M. D. BRYANT and G. K. HARITOS, *ASME J. Lubrication Technol.* **104** (1982) 347.
7. L. J. GHOSN, *J. Tribology* **110** (1988) 408.
8. H. C. SIN and N. P. SUH, *J. Appl. Mech.* **51** (1984) 317.
9. F. ERDOGAN and G. C. SIH, *J. Basic Enging* **85** (1963) 519.
10. G. C. SIH, *Int. J. Fracture* **10** (1974) 305.
11. S. JAHANMIR, N. P. SUH and E. P. ABRAHAMSON, *Wear* **26** (1974) 235.
12. K. SADEGHIPOUR, W. CHEN and G. BARAN, *J. Physics D: Appl. Phys.* **27** (1994) 1300.
13. Automatic Dynamic Incremental Nonlinear Analysis (ADINA), Version 6.1, ADINA R& D, Inc. (Watertown, MA, 1992).

Received 4 July and accepted 21 December 1995